Int J Cardiovasc Imaging (2013) 29:545–551
DOI 10.1007/s10554-012-0114-5

ORIGINAL PAPER

Right ventricular regional and global systolic function is diminished in patients with pulmonary arterial hypertension: a 2-dimensional ultrasound speckle tracking echocardiography study

Yuman Li · Mingxing Xie · Xinfang Wang · Qing Lu · Manli Fu

Received: 6 December 2011 / Accepted: 26 July 2012 / Published online: 6 September 2012

Abstract The purpose of the study is to evaluate right ventricular (RV) regional and global systolic function in patients with pulmonary arterial hypertension (PAH) by 2-dimensional ultrasound speckle tracking echocardiography (STE) and explore the impact of pulmonary artery systolic pressure (PASP) and pulmonary vascular resistance (PVR) on RV systolic function. 42 patients with PAH and 31 healthy controls were included in this study. RV longitudinal peak systolic strain (LS) and strain rate (LSRs) were measured at the basal, mid and apical segments of the RV free wall and septum by STE. RV global longitudinal peak systolic strain (GLS) and strain rate (GLSRs) were also measured by STE. RV ejection fraction (EF) was determinated by cardiac magnetic resonance (CMR) imaging. LS and LSRs of RV 6 segments were significantly reduced in patients with PAH compared with controls. RV GLS and GLSRs were lower in patients with varying degrees of PAH than controls. Furthermore, RV GLS were most altered in patients with severe PAH compared with mild PAH. PVR was correlated with RV GLS and GLSRs ($r_1 = -0.549$; $r_2 = -0.466$, respectively, $P < 0.05$). Similarly, there was correlation between PASP and RV GLS and GLSRs ($r_1 = -0.551$; $r_2 = -0.425$, respectively, $P < 0.05$). GLS and GLSRs were correlated with CMR-derived RVEF. ($r_1 = 0.693$; $r_2 = 0.560$, respectively, $P < 0.05$). STE can identify impaired RV regional and global systolic function in patients with PAH. STE-derived strain and strain rate can be used as novel indices for RV function assessment from 2-dimensional echocardiographic images.

Keywords Echocardiography · Pulmonary hypertension · Right ventricular function · 2-dimensional speckle tracking

Y. Li · M. Xie (✉) · X. Wang · Q. Lu · M. Fu
Hubei Provincial Key Laboratory of Molecular Imaging, Department of Ultrasonography, Union Hospital of Tongji Medical College, Huazhong University of Science and Technology, 1277# Jiefang Ave, Wuhan 430022, China
e-mail: xiemx64@126.com

Introduction

Pulmonary arterial hypertension (PAH) is characterized by the sustained increase in pulmonary vascular resistance (PVR) and pulmonary artery pressure, which if untreated, leads to right heart failure and death. Right ventricular (RV) dysfunction is the independent predictor of a poor prognosis in a variety of cardiopulmonary diseases [1].Therefore, evaluation of RV function in patients with PAH has increased in clinical importance. Owing to the complex geometry of the right ventricle, the conventional 2-dimensional measurements of RV volumes and functions can be considered less accurate. Cardiac magnetic resonance (CMR) imaging is the gold standard for evaluating the RV volume and ejection fraction, however, it is inapplicable in certain patients (e.g. with claustrophobia or implanted metallic devices). In addition, its wide use is precluded by cost, long scan and analysis time, limited availability, and dedicated expertise.

Recently, strain and strain rate imaging derived from tissue Doppler imaging (TDI) is widely used in evaluating left and right ventricular function [2–4], though TDI has an intrinsic limitation of angle-dependence, the angle-dependent method could less accurately assess myocardial performance. In this study, we present a novel technique based on speckle tracking that enables the accurate quantitative assessment of myocardial function. Speckle tracking echocardiography (STE) quantitatively analyzes the

displacement and velocity of the myocardium by tracking myocardial movement from frame to frame throughout the cardiac cycle, and affords a new method to assess global and regional myocardial function [5–7]. Accordingly, we sought to test the hypotheses that RV regional and global systolic function was reduced in patients with PAH and that pulmonary artery systolic pressure (PASP) and PVR directly affected RV systolic function. We also hypothesized that these changes in RV systolic function will be more marked in the severe than mild PAH group.

Methods

Study population

From October 2009 to February 2011,we included 42 patients with chronic PAH who had evidence of PAH defined as peak PASP >35 mm Hg estimated by Doppler echocardiography [8]. Among all the patients with PAH, 21 patients presented with idiopathic PAH, 17 with connective tissue diseases, 4 with Eisenmenger's disease. Exclusion criteria were: pulmonary artery stenosis or RV outflow tract obstruction, tricuspid structural disease, RV pacing, RV myocardial infarction, or idiopathic cardiomyopathy. According to PASP, a total of 42 patients with PAH were divided into mild (36–49 mmHg), moderate (50–70 mmHg) and severe (>70 mmHg) PAH groups [9]. The control group consisted of 31 age- and sex-matched normal subjects who had no cardiopulmonary disease through physical check-up, electrocardiogram, chest X-ray and echocardiography. All subjects were determined to be in sinus rhythm. The study was approved by an institutional review committee and all the subjects gave informed consent.

Echocardiographic equipment and conventional echocardiographic parameters

Echocardiography was performed using a commercially available ultrasound transducer and equipment (M3S probe, Vivid 7; GE Medical Systems, Horten, Norway) with subjects at rest in the left lateral decubitus position. All images were digitally stored for off-line analysis (EchoPAC, version BT06; GE-Vingmed, Norway). RV end-diastolic diameter (RVEDD) was determinated from the apical 4-chamber view [10]. For conventional RV function echocardiographic assessment, the tricuspid annular peak systolic velocity (Sm), early diastolic velocity (Em) and late diastolic velocity (Am) were measured by TDI from the apical 4-chamber view at the RV free wall level [10]. RV end-diastolic and end-systolic areas were also measured from the same view to calculate RV fractional area change (RVFAC) [10]. An index of PVR was derived by dividing the maximal velocity of the tricuspid regurgitant (TR) jet by the RV outflow tract time–velocity integral (VTI_{RVOT}), as previously described [11]. PASP was estimated from the peak continuous-wave Doppler velocity of the TR jet, using the modified Bernoulli equation plus right atrial pressure estimated from the inferior vena caval size and collapsibility with respiration, as previously validated and described by others [10].

2-dimensional STE processing

Two dimensional grayscale images of subjects at a frame rate of 60–90 frames/s were obtained from the apical 4-chamber view, 3 consecutive cardiac cycles were acquired and digitally stored for offline analysis. RV endocardial border was manually traced in the end-systolic frame when endocardial border is the clearest during the cardiac cycle. Regional of interest (ROI) in each image was automatically generated. The position of ROI and its width was adjusted manually when the speckle tracking appeared to be poor. The software then automatically tracked and accepted segments of good tracking quality and rejected poorly tracked segments. When all segments of RV were accepted, the regional longitudinal strain curves were obtained for 6 RV segments (the basal, mid, and apical segments of the RV free wall and septum), and the global RV strain curve was based on the average of the 6 regional strain curves. Representative examples of regional and global longitudinal strain and strain rate curves taken from the right ventricle by STE were shown in Fig. 1.

CMR imaging

A subset of 20 randomly selected patients with PAH was also studied with CMR imaging to assess RV ejection fraction (RVEF) and volumes within 7 days of echocardiography. A 1.5-T MRI (Magnetom Avanto, Siemens Healthcare, Erlangen, Germany) was applied, and consecutive single-slice acquisitions from base to apex of right ventricle in standard short-axis orientation were obtained, using a retrospectively ECG gated cine SSFP sequence [TR 39.75 ms, TE1.12 ms, slice thickness 6–8 mm, FOV 320–400 mm^2 (according to the individual size), matrix 156 × 192, bandwidth 930, flip angle 80°, average 1]. Image datasets were transferred to computer workstation and analysed by a single experienced observer blinded to echocardiographic results, using dedicated software (Argus). End-diastolic and end-systolic contours were manually traced for each slice in the short-axis view. RV end-diastolic volume (RVEDV) and end-systolic volume (RVESV) and RVEF was automatically obtained from the above analysis.

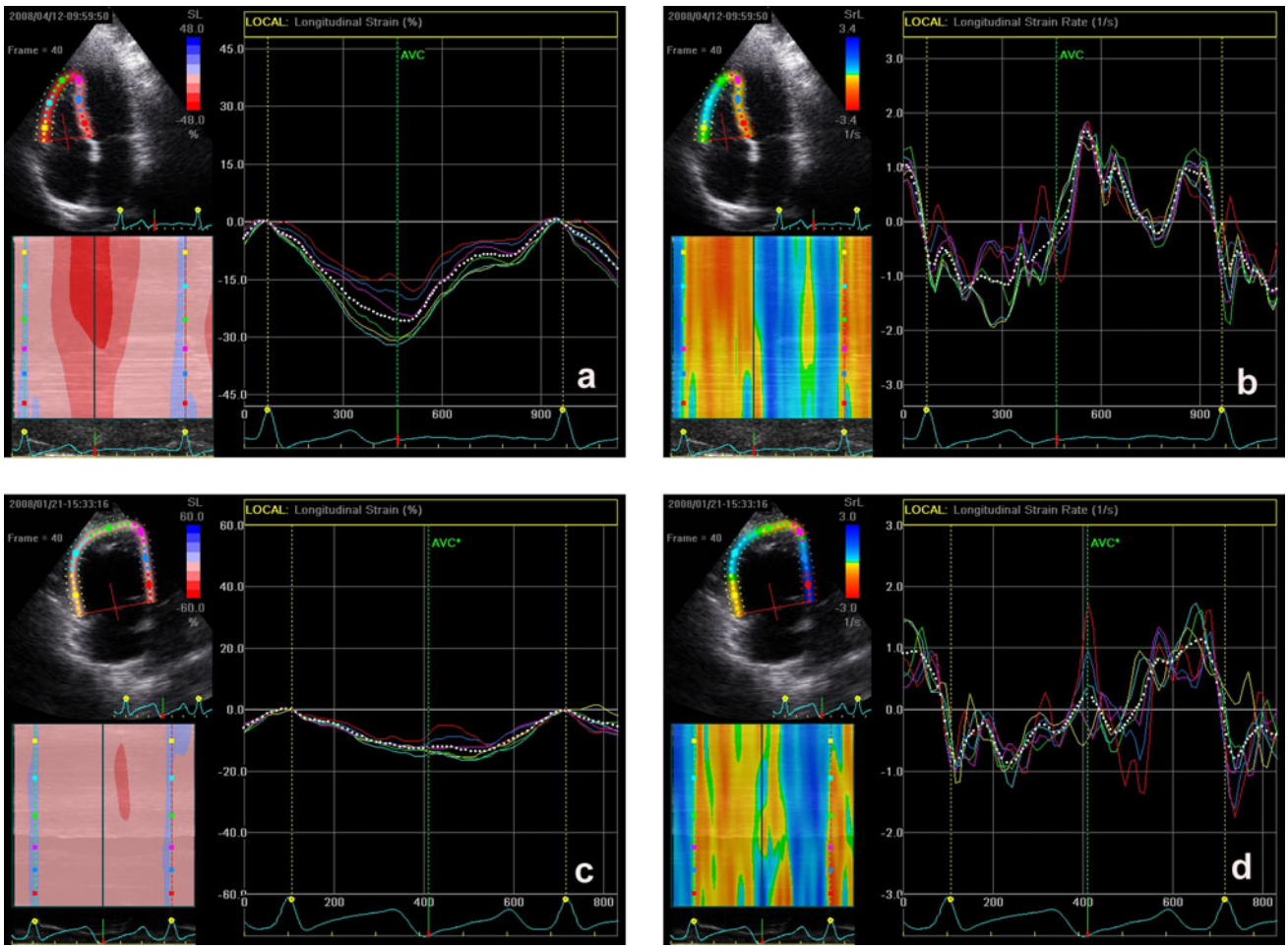

Fig. 1 RV regional (*different color curves*) and global longitudinal strain curves (*white dotted curves*) in normal control (**a**) and in patient with PAH (**c**). RV regional (*different color curves*) and global longitudinal strain rate curves (*white dotted curves*) in normal control (**b**) and in patient with PAH (**d**)

Statistical analysis

Statistical analysis was performed with a SPSS software package (SPSS for Windows 11.5). Continuous data were expressed as mean value ± standard deviation (SD). Comparison between the PAH and control groups was made with Student's t tests. Further comparison among the mild, moderate and severe PAH groups were made with 1-way analysis of variance with Bonferroni's post hoc analysis. The correlation between RV global systolic function and hemodynamic parameters was calculated as Pearson's coefficient. Within the patient cohort, Pearson correlation analysis was also used to assess the relations between RVGLS and GLSRs and CMR-derived RV volumes and EF. For all analyses, a value of $P < 0.05$ was considered as statistically significant.

Intraobserver and interobserver variability were assessed in randomly selected 16 subjects (5 patients with PAH and 11 normal controls), intraobserver variability was determined by having one observer remeasurement after 1 month. Interobserver variability was determined by a second observer who was blinded to the clinical and the STE findings. Interobserver and intraobserver reproducibility were evaluated by means of intraclass correlation coefficient (ICC) and Bland–Altman analysis.

Results

Speckle tracking strain analysis

In our study, 6 patients with PAH and 3 controls were excluded owing to poor 2-dimensional image of apical 4-chamber view during the image acquisition. During the image analysis, 9 patients with PAH and 6 controls with images of inadequate quality for optimal speckle tracking were excluded. Reliable measurements were obtained in 74 % of patients (42 of 57) with PAH and 78 % of control subjects (31 of 40).

Baseline characteristics

Baseline characteristics of the study population were shown in Table 1. Sm and RVFAC were significantly lower in the moderate and sever PAH group than the control group. The PAH group had large RV, and increased PVR. Further comparison among patients with mild, moderate and severe PAH yielded a gradual decrease in Sm and RVFAC with worsening PAH. However, there were no significant differences in Em and Am among the mild, moderate and severe PAH groups.

RV regional longitudinal function

LS and LSRs of RV 6 segments in normal controls and patients with PAH were shown in Fig. 2. Compared with normal controls, LS of the basal, mid, and apical segments of the RV free wall and septum were reduced in patients with PAH ($P < 0.05$ for all). Similarly, LSRs of RV 6 segments were also lower in PAH than control group ($P < 0.05$ for all).

RV global longitudinal function

RV GLS and GLSRs in control and PAH groups were shown in Fig. 2. Further comparisons among the varying degrees of PAH group were shown in Fig. 3. Compared with normal controls, RVGLS and GLSRs were significantly reduced in patients with varying degrees of PAH ($P < 0.05$ for all). Comparison with mild PAH group, RVGLS was decreased further in severe PAH group (-14.22 ± 4.93 % in severe PAH vs. -20.52 ± 5.60 % in mild PAH, $P < 0.05$). There were no significant differences in GLSRs among the mild, moderate and severe PAH groups ($P > 0.05$ for all). There were moderate correlations between Sm and RV GLS($r = 0.556$, P = 0.000) and GLSRs ($r = 0.585$, $P = 0.000$) in patients with PAH.

The relationship between RV global function and hemodynamic parameters

The correlations between RV global function and the conventional 2D and doppler echocardiographic, and TDI

Table 1 General characteristics of the controls and patients with PAH

Variable	Control group (n = 31)	Mild PAH group (n = 17)	Moderate PAH group (n = 15)	Severe PAH group (n = 10)
Female	19 (61 %)	11 (65 %)	10 (67 %)	6 (60 %)
Age (years)	37 ± 14	41 ± 18	34 ± 13	40 ± 24
HR (beats/min)	77 ± 10	77 ± 8	75 ± 6	80 ± 11
RVEDD (cm)	3.24 ± 0.51	4.16 ± 0.85*	4.23 ± 0.78*	4.77 ± 0.87*$^{\triangle}$
RVFAC (%)	51.66 ± 10.54	45.34 ± 14.11	37.30 ± 8.38*$^{\triangle}$	31.67 ± 7.80*$^{\triangle}$
Sm (cm/s)	10.36 ± 1.74	9.61 ± 3.28	8.53 ± 2.17*	6.78 ± 3.13*$^{\triangle}$
Em (cm/s)	−8.38 ± 4.06	−9.27 ± 2.90	−8.33 ± 3.38	−9.55 ± 5.11
Am (cm/s)	−8.35 ± 2.11	−9.77 ± 2.69	−7.78 ± 5.06	−8.80 ± 4.21
PVR (s^{-1})	8.23 ± 3.73	23.45 ± 13.83*	29.59 ± 14.19*	67.55 ± 22.79*$^{\triangle\blacktriangle}$
PASP (mmHg)	19.66 ± 5.51	42.97 ± 4.62*	64.85 ± 5.10*$^{\triangle}$	100.85 ± 14.28*$^{\triangle\blacktriangle}$

HR heart rate; RVFAC: RV fractional area change; RVEDD:RV end-diastolic diameter; Sm: tricuspid annular peak systolic velocity; Em: tricuspid annular peak early diastolic velocity; Am: tricuspid annular peak late diastolic velocity; PVR: pulmonary vascular resistance; PASP: pulmonary artery systolic pressure; * $P < 0.05$ compared with normal controls; $^{\triangle}$ $P < 0.05$ compared with patients with mild PAH. $^{\blacktriangle}$ $P < 0.05$ compared with patients with moderate PAH

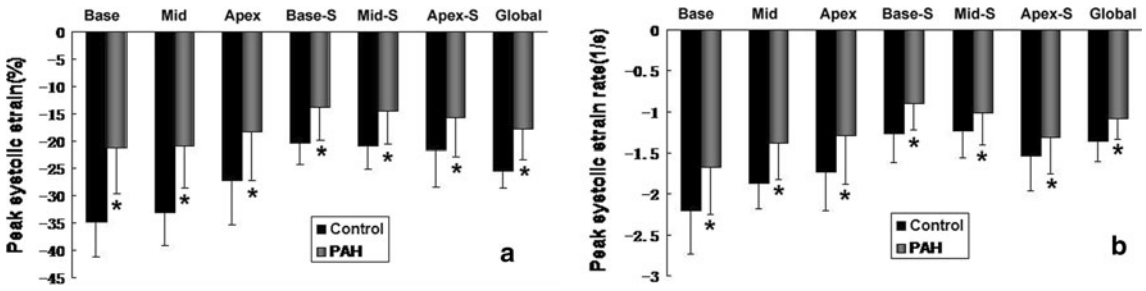

Fig. 2 RV segmental and global LS (**a**) and LSRs (**b**) in the control and PAH groups. Base: basal RV free wall; Mid: mid RV free wall; Apex: apical RV free wall; Base-S: basal septum; Mid-S: mid septum; Apex-S: Apical septum. *$P < 0.05$ versus the control group

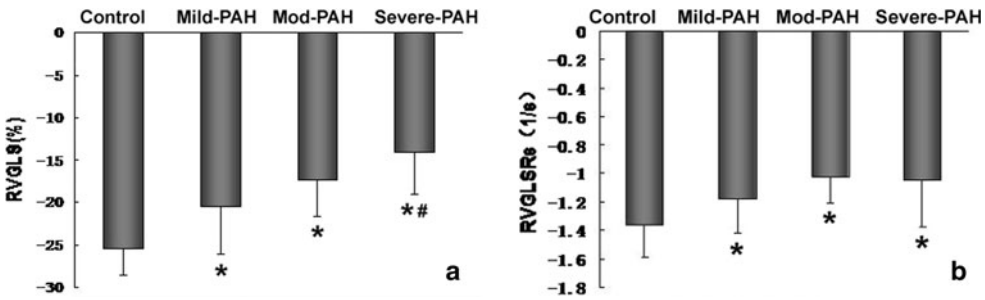

Fig. 3 RVGLS (**a**) and GLSRs (**b**) in the control and the mild, moderate and severe PAH groups. $^{*}P < 0.05$ versus the control group; $^{\#}P < 0.05$ versus the mild PAH group

Table 2 Other parameters in correlation with RV global longitudinal strain and strain rate

Variable	GLS (%)		GLSRs (S^{-1})	
	R value	*P* value	*R* value	*P* value
PVR (S^{-1})	−0.549	0.000	−0.466	0.002
PASP (mmHg)	−0.551	0.000	−0.425	0.006
RVEDD (cm)	−0.052	0.744	−0.109	0.492
Sm (cm/s)	0.556	0.000	0.585	0.000

PVR pulmonary vascular resistance, *PASP* pulmonary artery systolic pressure, *RVEDD* RV end-diastolic diameter; Sm: tricuspid annular peak systolic velocity

parameters were listed in Table 2. PVR was correlated significantly with RV GLS and GLSRs ($r_1 = -0.549$; $r_2 = -0.466$, respectively, $P < 0.05$) (Fig. 4a, b). Similarly, there was significant correlation between PASP and RV GLS and GLSRs ($r_1 = -0.551$; $r_2 = -0.425$ respectively, $P < 0.05$) (Fig. 4c, d). But no significant correlations were found between RV GLS and RVEDD, and between GLSRs and RVEDD.

Correlations between RV echocardiographic and CMR parameters

The CMR findings in the 20 patients were as follows: RVEDV (116.5 ± 36.9) ml, RVESV (41.8 ± 25.8) ml and RVEF (51.8 ± 13.6) %. We also found the relationship between RVGLS and GLSRs and CMR parameters in a subset of 20 patients with PAH (Fig. 4e, f). Both RVGLS and GLSRs were significantly correlated with RVEF ($r_1 = 0.693$; $r_2 = 0.560$, respectively, $P < 0.05$), and not with RVEDV and RVESV. On the other hand, relation between Sm and RVEF was also investigated in our study ($r = 0.506$, $P = 0.003$).

Intraobserver and interobserver variability

By Bland–Altman analysis, the limits of agreement for interobserver reproducibility were −2.3 to 2.7 % for GLS and −0.16 to 0.20 S^{-1} for GLSRs, and the limits of agreement for intraobserver reproducibility were −4.5 to 3.6 % and −0.3 to 0.33 S^{-1} for GLS and GLSRs. The interobserver ICC was 0.93 for GLS and 0.93 for GLSRs, and the intraobserver ICC was 0.95 and 0.93 for GLS and GLSRs.

Discussion

This study demonstrates that RV regional and global systolic functions are lower in patients with PAH than normal controls. Furthermore, impaired RV contractility is marked in severe compared with mild PAH group. RV GLS and GLSRs correlate with hemodynamic parameters. RV GLS and GLSRs are also correlated with CMR-derived RVEF. We conclude that chronic RV pressure overload directly affects RV systolic performance.

RV muscle bands are mostly made up of longitudinal superficial spatial muscle. In the systole, cardiac base of the right ventricle moves towards cardiac apex and forwards the interventricular septum [12]. Therefore, we assess mainly RV longitudinal systolic function when assessing RV systolic function. The conventional RV function parameters, such as tricuspid annular plane systolic excursion (TAPSE) and Sm, are widely used in clinical practice and can be considered validated indices of global RV contractility [10]. But, they have a number of limitations, such as angle- dependence. These parameters provide information about RV global function and do not afford important regional changes in myocardial performance. For RV global function assessment, TAPSE and Sm assume that the function of a single segment represent the function of the entire right ventricle, while STE-derive global strain and strain rate were based on the average of the RV 6 segmental strain and strain rate. Therefore, STE-derived indices are superior to Sm and RVFAC, because they not only allow the regional analysis of RV contractility and contraction synchronicity, but also allow the global analysis of RV function [13–15]. In our study, Sm and RVFAC were only lower in the moderate and sever PAH group than the control group, while STE-derived GLS and GLSRs were reduced in mild, moderate and sever PAH compared with control group. Sm and RVFAC failed to differentiate patients with mild PAH from normal controls.

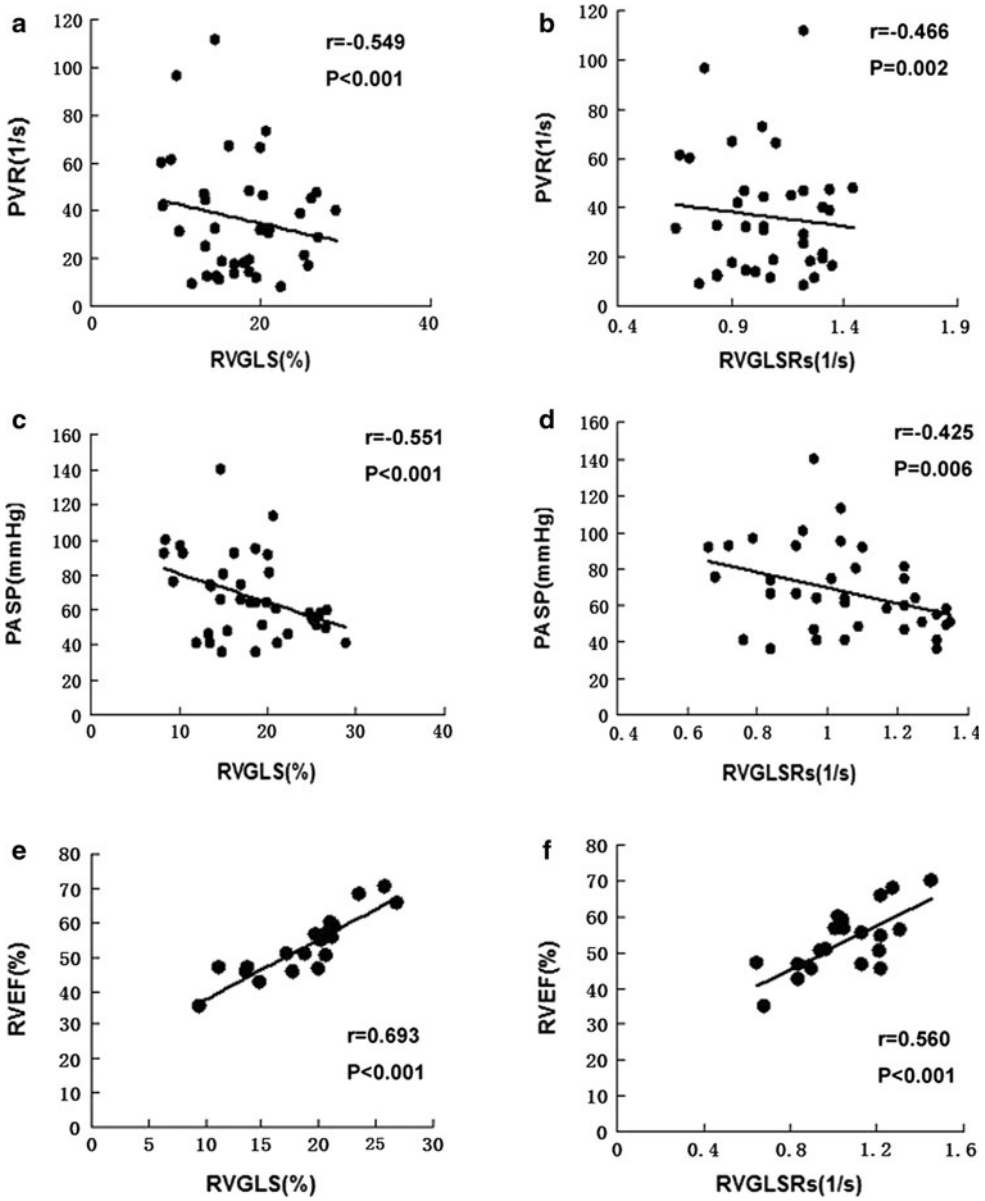

Fig. 4 Correlations between PVR and RVGLS (**a**) and GLSRs (**b**), relation between PASP and RVGLS (**c**) and GLSRs (**d**), and relationship between CMR-derived RVEF and RVGLS (**e**) and GLSRs (**f**)

In the study we found that RV free wall and interventricular septal LS and LSRs were decreased in patients with PAH compared with normal controls. These findings were in accordance with previous studies [9, 16–19]. Meris et al. [17] and Puwanant et al. [18] investigated RV free wall and IVS LS measured by STE were impaired in patients with PAH compared with normal subjects. Pirat et al. [9] showed that RV free wall and IVS LS and LSRs mearsured by Velocity Vector Imaging were reduced in patients with PAH compared with normal controls. But, none of the above prevous study test the utility of STE-derived GLS and GLSRs for RV global function assessment in patients with varying degrees of PAH. In the present study, we investigated that RV global strain and strain rate were lower in patients with varying degrees of PAH than in normal subjects, furthermore, patients with mild, moderate and severe PAH yielded a gradual decrease in all parameters with worsening PAH. RV GLS could differentiate patients with mild PAH from those with severe PAH. Moreover, our study also showed that RV GLS and GLSRs were significantly correlated with PVR and PASP. Pirat et al. [9] and Puwanant et al. [18] also found RV regional LS correlated with PASP and PVR.

Our study demonstrates that RV global strain and stain rate correspond with CMR-derived RVEF; these are in agreement with prior study [16]. Moreover, we also observe that Sm is correlated with RVEF, but correlation coefficient is lower than the former. Prior study also

demonstrated that Sm was positively correlated with RVEF [20]. We conclude that STI-derived RV strain and strain rate can be used as novel indices for assessment of RV systolic function from 2-dimensional echocardiographic images. Furthermore, STE-derived RV global longitudinal strain and strain rate for RV function assessment are superior to Sm.

Study limitations

Our study has potential limitations. First of all, this study include a small number of patients, future studies of larger samples needs to determine the utility of STE–derived strain and strain rate for the assessment of RV myocardial function. In addition, we assess RV function merely by the apical 4-chamber view because that RV acoustic window is limited. Third, not all patients underwent CMR imaging. Therefore, relationship between RV global strain and strain rate and RV function by CMR imaging need to be further assessed.

Finally, mix of patients with various type of PAH is a limitation. Although the pathophysiology of PAH differs between idiopatic, connective tissue diseases and Einsenmenger PAH, eventually these diseases result in RV pressure overload. Whereas we focus on the impact of RV pressure overload on RV systolic function.

Conclusions

STE can identify abnormalities in RV regional and global systolic function in patients with varying degrees of PAH. STE is a new simple, valid, and reproducible method to assess RV systolic function from standard bidimensional images.

Conflict of interest None.

References

1. Voelkel NF, Quaife RA, Leinwand LA et al (2006) Right ventricular function and failure: report of a National Heart, Lung, and Blood Institute working group on cellular and molecular mechanisms of right heart failure. Circulation 14:1883–1891
2. Di Salvo G, Drago M, Pacileo G et al (2005) Comparison of strain rate imaging for quantitative evaluation of regional left and right ventricular function after surgical versus percutaneous closure of atrial septal defect. Am J Cardiol 96:299–302
3. Weidemann F, Eyskens B, Mertens L et al (2002) Quantification of regional right and left ventricular function by ultrasonic strain rate and strain indexes after surgical repair of tetralogy of Fallot. Am J Cardiol 90:133–138
4. Pedrinelli R, Canale ML, Giannini C et al (2010) Right ventricular dysfunction in early systemic hypertension: a tissue Doppler imaging study in patients with high-normal and mildly increased arterial blood pressure. J Hypertens 28:615–621
5. Artis NJ, Oxborough DL, Williams G et al (2008) Two-dimensional strain imaging: a new echocardiographic advance with research and clinical applications. Int J Cardiol 123:240–248
6. Han W, Xie MX, Wang XF et al (2008) Assessment of left ventricular torsion in patients with anterior wall myocardial infarction before and after revascularization using speckle tracking imaging. Chin Med J 121:1543–1548
7. Perk G, Tunick PA, Kronzon I (2007) Non-Doppler two-dimensional strain imaging by echocardiographȳfrom technical considerations to clinical applications. J Am Soc Echocardiogr 20:234–243
8. Currie PJ, Seward JB, Chan KL et al (1985) Continuous wave Doppler determination of right ventricular pressure: a simultaneous Doppler-catheterization study in 127 patients. J Am Coll Cardiol 6:750–756
9. Pirat B, McCulloch ML, Zoghbi WA (2006) Evaluation of global and regional right ventricular systolic function in patients with pulmonary hypertension using a novel speckle tracking method. Am J Cardiol 98:699–704
10. Rudski LG, Lai WW, Afilalo J et al (2010) Guidelines for the echocardiographic assessment of the right heart in adults: a report from the American Society of Echocardiography endorsed by the European Association of Echocardiography, a registered branch of the European Society of Cardiology, and the Canadian Society of Echocardiography. J Am Soc Echocardiogr 23:685–713
11. Abbas AE, Fortuin FD, Schiller NB et al (2003) A simple method for noninvasive estimation of Pulmonary vascular resistance. J Am Coll Cardiol 41:1021–1027
12. Torrent-Guasp F, Ballester M, Buckberg GD et al (2001) Spatial orientation of the ventricular muscle band: physiologic contribution and surgical implications. J Thorac Cardiovasc Surg 122:389–392
13. Cho GY, Marwick TH, Kim HS et al (2009) Global 2-dimensional strain as a new prognosticator in patients with heart failure. J Am Coll Cardiol 54:618–624
14. Reisner SA, Lysyansky P, Agmon Y et al (2004) Global longitudinal strain: a novel index of left ventricular systolic function. J Am Soc Echocardiogr 17:630–633
15. Donal E, Tournoux F, Leclercq C et al (2008) Assessment of longitudinal and radial ventricular dyssynchrony in ischemic and nonischemic chronic systolic heart failure: a two-dimensional echocardiographic speckle-tracking strain study. J Am Soc Echocardiogr 21:58–65
16. Fukuda Y, Tanaka H, Sugiyama D et al (2011) Utility of right ventricular free wall speckle-tracking strain for evaluation of right ventricular performance in patients with pulmonary hypertension. J Am Soc Echocardiogr 24:1101–1108
17. Meris A, Faletra F, Conca C et al (2010) Timing and magnitude of regional right ventricular function: a speckle tracking-derived strain study of normal subjects and patients with right ventricular dysfunction. J Am Soc Echocardiogr 23:823–831
18. Puwanant S, Park M, Popović ZB et al (2010) Ventricular geometry, strain, and rotational mechanics in pulmonary hypertension. Circulation 121:259–266
19. Borges AC, Knebel F, Eddicks S et al (2006) Right ventricular function assessed by two-dimensional strain and tissue doppler echocardiograhy in patients with pulmonary arterial hypertension and effect of vasodilator therapy. Am J Cardiol 98:530–534
20. Rajagopalan N, Saxena N, Simon MA et al (2007) Correlation of tricuspid annular velocities with invasive hemodynamics in pulmonary hypertension. Congest Heart Fail 13:200–204